AGU100 ADVANCING EARTH AND SPACE SCIENCE

Geophysical Research Letters

RESEARCH LETTER
10.1029/2019GL082792

Ice and Permafrost Effects on Delta Morphology and Channel Dynamics

Rebecca Lauzon[1,2], Anastasia Piliouras[1], and Joel C. Rowland[1]

[1]Earth and Environmental Science Division, Los Alamos National Laboratory, Los Alamos, NM, USA, [2]Division of Earth and Ocean Sciences, Nicholas School of the Environment, Duke University, Durham, NC, USA

Key Points:
- Ice cover and permafrost decrease channel mobility, increase shoreline roughness, and route more sediment offshore on Arctic river deltas
- Water level backup upstream of ice cover enhances flooding and overbank deposition on Arctic river deltas
- Permafrost and ice loss may limit delta storage and alter the timing and magnitude of fluxes of water, sediment, and nutrients to the coast

Supporting Information:
- Supporting Information S1
- Table S1
- Movie S1
- Movie S2
- Movie S3
- Movie S4
- Movie S5
- Movie S6
- Movie S7
- Movie S8
- Movie S9
- Movie S10

Correspondence to:
R. Lauzon,
beccalauzon@gmail.com

Citation:
Lauzon, R., Piliouras, A., & Rowland, J. C. (2019). Ice and permafrost effects on delta morphology and channel dynamics. *Geophysical Research Letters*, *46*, 6574–6582. https://doi.org/10.1029/2019GL082792

Received 11 MAR 2019
Accepted 31 MAY 2019
Accepted article online 6 JUN 2019
Published online 19 JUN 2019

Abstract Arctic regions are changing rapidly as permafrost thaws and sea ice retreats. These changes directly affect Arctic river deltas, but how permafrost and ice alter delta hydrology and sediment transport are not well researched. This knowledge gap limits our ability to forecast how these systems will respond to continued warming. We adapt the reduced complexity model of delta morphodynamics DeltaRCM to investigate the influences of permafrost and landfast ice on delta morphology and channel dynamics. We find that ice cover and permafrost decrease channel mobility, increase shoreline roughness, and route and deposit more sediment offshore. Ice cover also enhances overbank deposition, increasing subaerial delta elevations. Our modeling suggests that permafrost and ice loss in a warming climate could lead to less overbank and offshore deposition and more dynamic and spatially distributed fluxes of water and sediment across Arctic river deltas.

Plain Language Summary Arctic regions are warming rapidly, causing frozen soils to thaw and sea ice to melt. These changes directly affect Arctic river deltas that connect the continents to the Arctic Ocean. Because of the difficulty of research in these remote regions, we do not yet understand how ice cover and frozen soil (i.e., permafrost) affect coastal change, which limits our ability to predict coastal dynamics in a warming environment. This study uses a numerical model to examine the impacts of ice cover and permafrost on Arctic delta dynamics. We found that both ice and permafrost make channels more stable. Ice fills channels and forces flow underneath the ice, preserving channels that would otherwise be filled with sediment over time. This also causes increased delivery of sand and mud to the coastal ocean. Ice cover enhances vertical delta growth by encouraging flooding, implying that a reduction in ice cover resulting from warming will result in less vertical delta growth and therefore less of an ability to keep up with sea level rise. Our results also suggest that loss of permafrost and ice may result in more mobile channels, which will fundamentally change how rivers deliver water, sediments, and nutrients to the coastal ocean.

1. Introduction

The Arctic is experiencing accelerated warming (Intergovernmental Panel on Climate Change, 2013), permafrost thaw (Arctic Climate Impact Assessment, ACIA, 2004; Jorgenson et al., 2006; Lachenbruch & Marshall, 1986; Slater & Lawrence, 2013), sea ice retreat (ACIA, 2004; Barnhart et al., 2016; Overeem et al., 2011; Simmonds, 2015), and sea level rise (ACIA, 2004; Proshutinsky et al., 2001). Arctic river deltas are particularly susceptible to climate change, but these remote landforms remain poorly studied compared to their temperate counterparts. Arctic deltas are ice covered for 7–9 months a year and underlain by varying extents of permafrost. How future permafrost loss and changes in ice thickness and extent will alter the structure and function of Arctic deltas is a fundamental unanswered question. Reworking of Arctic delta floodplains will release vast stores of carbon (Gustafsson et al., 201; Rowland et al., 2010) into the atmosphere or ocean, making it important to understand how Arctic deltas will respond to a warming climate.

Frozen pore waters can greatly increase soil strength over that of unfrozen materials (Tsytovich, 1975; Williams & Smith, 1991) and frozen banks must thaw prior to being physically eroded. Both effects may slow erosion rates in permafrost systems. Additionally, permafrost makes erosion rates sensitive to climate-driven changes in hydrology and temperature (Dupeyrat et al., 2011; Randriamazaoro et al., 2007). On deltas, thawing permafrost may increase channel mobility, land subsidence, and thermokarst lake creation and expansion (Rowland et al., 2010; Williams & Smith, 1991), which all affect fluxes of water, sediment, and nutrients through deltas.

Free-floating and landfast (i.e., attached to land) ice are both present on Arctic deltas and affect water flow through channels by introducing friction (resistance) at the ice-water interface (Lotsari et al., 2017; Smith & Ettema, 1997; Sui et al., 2010; Toniolo et al., 2013; Wang et al., 2008). For free-floating ice, this decreases velocities (Lotsari et al., 2017; Smith & Ettema, 1997; Sui et al., 2010), which reduces bed shear stresses and sediment transport (Lau & Krishnappan, 1985; Smith & Ettema, 1997). For landfast ice, friction moves maximum velocities closer to the bed (Lotsari et al., 2017; Sui et al., 2010; Wang et al., 2008) and flow constriction under the ice increases velocities (Lotsari et al., 2017; Robert & Tran, 2012). This suggests that landfast ice may enhance below-ice sediment transport, however, to our knowledge, this has not been confirmed by data. This hypothesis suggests that landfast ice, present on Arctic river deltas during spring snowmelt floods (Walker, 1998), may have a larger impact on delta dynamics than floating ice.

Using the reduced complexity model of delta morphodynamics DeltaRCM (Liang, Geleynse, et al., 2015; Liang, Voller, & Paola, 2015; Liang, Kim, & Passalacqua, 2016; Liang, Van Dyk, & Passalacqua, 2016), we investigate the influences of permafrost and landfast ice on river delta morphology, growth, and channel dynamics. By simplifying physical processes for incorporation into this rule-based model (Murray, 2003), we gain insights into the processes and process interactions most important to Arctic river delta dynamics, which would be difficult to obtain through other methods (e.g., remote sensing or field observations). Here we show that ice and permafrost alter channel mobility and depositional patterns on Arctic river deltas, affecting delta morphology, sediment retention, and the distribution of flow and sediment across the delta.

2. Materials and Methods

DeltaRCM consists of a grid of square cells, each with an associated water discharge, water surface elevation, and bed elevation. In each time step, the model divides water discharge into parcels, which enter the grid through a fixed inlet channel and are routed by a weighted random walk, with weights determined by inertia (average downstream direction), gravity (water surface gradient), and flow resistance. The depth-averaged flow field and water surface profile are then updated, and the sediment parcels, set fractions of which represent mud and sand, are routed by a similar random walk weighted by water discharge. Bed elevations are updated based on sediment parcel paths and lateral sediment diffusion, and the next time step begins. We adapt DeltaRCM for Arctic environments by incorporating the effects of ice and permafrost. Our modifications are described in detail below and in the supporting information, and a complete description of the model can be found in Liang, Voller, and Paola (2015).

We characterize ice cover by maximum ice thickness ($h_{i,\max}$) and initial upstream ice extent (f_{ice}; fraction of the delta length that is ice covered at the start of each model year). The model assumes bankfull flow conditions (Liang, Voller, & Paola, 2015), which we assume occur entirely during the spring flood based on observations of punctuated geomorphic activity associated with spring floods in Arctic deltas (Walker & Hudson, 2003). We therefore model only the melting of ice during the spring flood.

At the beginning of each flood, the ice is at its maximum thickness (which may not exceed 99% of the cell's water depth, h) and upstream extent. Ice thickness increases linearly downstream from zero at the initial ice extent boundary (f_{ice}) to $h_{i,\max}$ over 10 grid cells to prevent abrupt increases in ice thickness. During the flood, ice in each cell melts (i.e., thins) during each time step according to the heat flux provided by the local discharge and a background rate representing atmospheric melting. The discharge-weighted melting per time step is calculated after Searcy et al. (1996). To represent atmospheric melting, we calculate the rate necessary to melt all the ice over the exact length of the spring flood and then impose melting at a fraction of this rate (Text S1).

We incorporate two main effects of ice into the model: (1) increasing resistance by adding friction and (2) when landfast, constricting flow, reducing water depths by forcing flow under the ice. Flow resistance (R_f) in DeltaRCM was originally depth (h) dependent: $\frac{1}{R_f} = \boldsymbol{h}^{\theta}$, where $\theta = 1$ for water and mud (assumed to follow the water parcels) and $\theta = 2$ for sand parcels (assumed to preferentially follow deeper flow paths). We modify this equation to include additional flow resistance and constriction from ice $\frac{1}{R} = \boldsymbol{h_{eff}}\left(\mathbf{1} - \frac{\boldsymbol{h_i}}{\boldsymbol{h}}\right)$, where h_i is ice thickness and $\boldsymbol{h_{eff}} = \boldsymbol{h} - \boldsymbol{h_i}$. This formulation has several advantages: (1) when $h_i = 0$, it reduces to the original equation and (2) the resistance introduced by the ice increases as both h_i and h_i/h increase, consistent with observations that roughness (and therefore resistance) along the ice water interface increases with ice

thickness (Attar & Li, 2012). We also use h_{eff} to calculate velocity, so that velocities under ice are higher for the same discharge because of the decreased water depth, consistent with observations of flow under fast ice (Lotsari et al., 2017; Robert & Tran, 2012).

Permafrost is developed over time as the delta grows and develops only on the delta, not in the ocean. Permafrost is defined as ground that maintains a temperature below freezing for a minimum of 2 years and therefore can only exist below the active layer (seasonal thaw layer). We assign an active layer thickness of 0.5 m. Each model grid cell is vertically divided into 0.05-m-thick layers in which we track the amount of time (in model years) layers of sediment have been below the active layer. Layers that have been below the active layer $\geq$2 model years are flagged as permafrost. We assume that sediment below the active layer freezes during its first year, such that we are modeling systems with rapid rates of permafrost development. Sediment layers within the active layer are assigned an age of 0. In each time step, we use this 3-D permafrost map to assign a binary designation to each horizontal cell as permafrost or nonpermafrost based on thickness of permafrost layers relative to channel depth and total deposit thickness (Text S2).

To represent the decreased erodibility of permafrost without implementing a complex thermal erosion model (Dupeyrat et al., 2011; Randriamazaoro et al., 2007), we characterize permafrost with a relative erodibility (E; always <1). We increase the erosion velocity threshold and decrease lateral sediment diffusion by this relative amount for permafrost cells. Lateral sediment diffusion (q_{s_lat}) is a function of local lateral slope (S) and sand flux (q_{s_loc}): $\boldsymbol{q_{s\_lat} = \alpha S q_{s\_loc}}$. We multiply the smoothing coefficient (α) by E, such that a permafrost cell contributes less sediment to its neighbors through lateral diffusion than a nonpermafrost cell.

We present three sets of experiments (ice thickness, ice extent, and permafrost erodibility) using a 120 × 240 cell grid with sediment inputs of 25% sand and 75% mud. We prescribed a flood length of 10 days (34 model time steps; each ~7 hr), assuming 10 bankfull flow days per year; analysis of daily discharge data for six major Arctic rivers suggests this is a reasonable assumption. We delayed implementation of permafrost or ice cover until 300 time steps to allow establishment of an initial channel network. We ran each experiment in triplicate for 5,000 time steps (approximately 150 years).

We first varied only $h_{i,\max}$, using $f_{\text{ice}} = 40\%$, and $h_{i,\max} = 0.5$, 1, 2, 3, 4, and 4.5 m. We then varied both $h_{i,\max}$ and f_{ice} to represent the flood occurring at different times during the spring season. For $h_{i,\max} = 0.5$, 2, and 4 m, we tested $f_{\text{ice}} = 0\%$ (ice present only in ocean), 40%, 80%, and 100% (entire delta is ice covered). Finally, we examined permafrost erodibilities $E = 0.5$, 0.65, 0.8, and 0.95. Model deltas with $E = 0.5$ consistently reached the edge of the model domain before the end of a run and are therefore not presented here (see Table S3 and Figures S3 and S4). Details of data analysis methods can be found in Text S3.

3. Channel Networks and Channel Dynamics

Permafrost limits lateral channel mobility and inhibits channel incision, as frozen sediment requires higher velocities to erode. In our experiments, this results in fewer channels on deltas with permafrost (3.14 ± 0.38 channels) than on deltas with no ice or permafrost (3.77 ± 0.38). Decreasing erodibility also results in more frequent channel switching (avulsions), as permafrost-bound channels cannot easily adjust to local changes in discharge through lateral migration or bed erosion, and more favorable slope or resistance gradients may exist outside of active channels. For a slight decrease in erodibility ($E = 0.95$ or 0.8), this results in a more mobile and spatially disperse channel network (Figures 1f, 1g, and 2a). However, as erodibility decreases ($E = 0.65$) and migration and incision of new channels become more difficult, existing channels become strong flow attractors, and attempted avulsions are short-lived, resulting in decreased channel mobility (Figures 1h and 2a) and entrenchment of existing channels.

Thick ice cover enhances channel persistence (Figures 1c, 1d, 2b, 2c, and S1) through two mechanisms. First, it constricts and accelerates flow, limiting aggradation in channel beds. Second, ice preserves channels through a positive feedback. Increased flow resistance limits water discharge and sediment deposition, which would fill the abandoned channel. Without discharge, the ice melts slowly, and continues to provide resistance to flow. Channel persistence then increases as abandoned channels are preserved as topographic lows (Figure 5i) and shallower channels are blocked by ice, focusing flow in existing, deeper channels that become entrenched under the ice (Figure 3e).

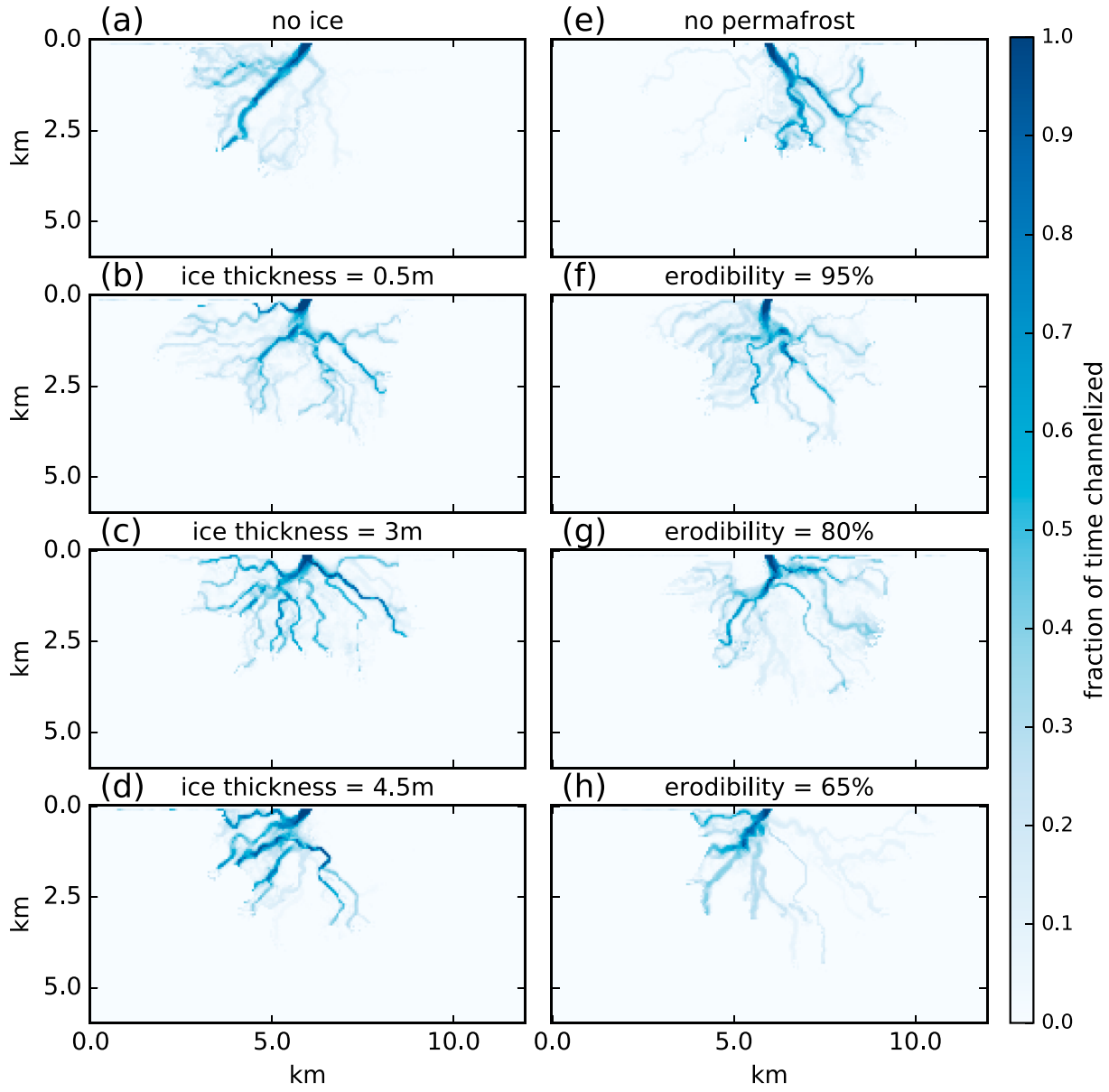

Figure 1. Maps showing the fraction of time each cell remained part of the channel network from t = 2,651–5,000 for example model runs. Panels (a) and (e) have no ice or permafrost. Ice thickness increases from (b) to (d) and permafrost erodibility decreases from (f) to (h).

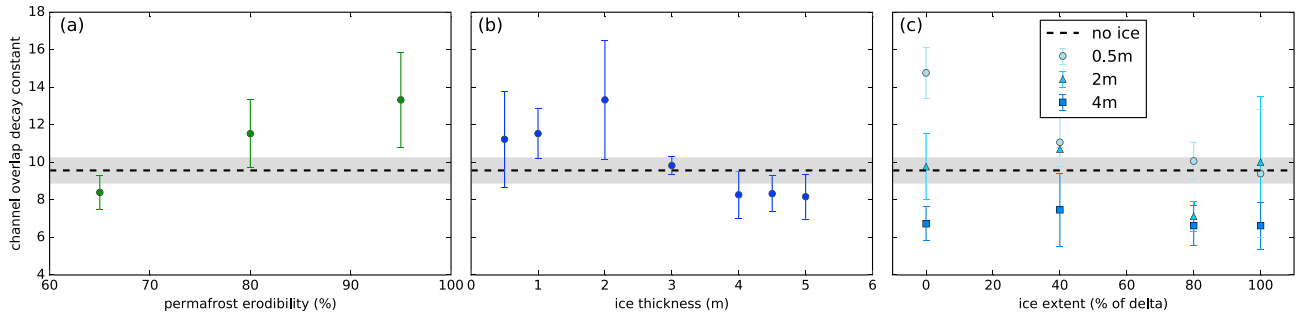

Figure 2. Decay in channel planform overlap (representing channel mobility) from t = 2,561–5,000 for (a) permafrost erodibility, (b) maximum ice thickness, and (c) maximum ice extent. Error bars represent one standard deviation. The dashed line represents the mean value for runs with no ice or permafrost, and the shading is one standard deviation.

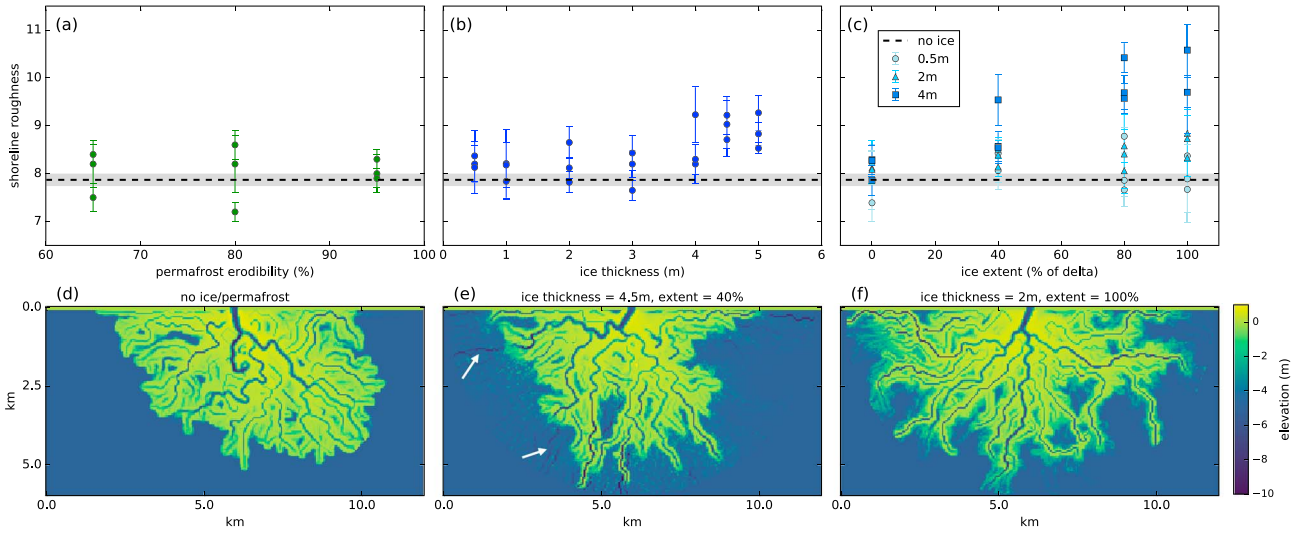

Figure 3. Mean shoreline roughness for (a) permafrost erodibility, (b) maximum ice thickness, and (c) maximum ice extent experiments. Error bars represent one standard deviation. Elevation maps for an example run with (d) no ice or permafrost, (e) a maximum ice thickness of 4.5 m and extent of 40% (arrows highlight incised channels), and (f) a maximum ice thickness of 2 m and extent of 100%.

This results in simulated deltas with ice cover having significantly more channels than deltas without ice for all ice thicknesses (4.47 ± 0.51, extent: 40%), but the mechanisms controlling the increase in channel number differ for thin and thick ice. On deltas with fast ice, water is forced under the ice, resulting in increased water levels upstream of the ice boundary (here termed "backup"; bottom right panel of Movies S6–S8). The resulting increase in water surface slope increases the likelihood of an avulsion. For thin ice cover (0.5 m), more avulsions result in increased channel mobility (Figure 2b) and in a spatially and temporally dynamic channel network distributed widely across the delta (Figure 1b), with more channels active at once than on deltas without ice. Channel mobility decreases with increasing ice extent for deltas with thin ice (Figure 2c) as more of the delta is ice covered, decreasing the number of possible flow paths with slope or resistance gradients favorable for avulsions.

For thick ice, increased velocities limit in-channel deposition and channel aggradation, which reduces the likelihood of avulsions despite backup creating favorable water surface slopes. When avulsions do occur, flow is more likely to reoccupy a preserved abandoned channel than to incise a new channel. This results in overall increased persistence in channel locations (Figure 1d) and decreased channel mobility (Figure 2b). Additionally, the channel network appears concentrated on only one part of the delta for thick ice runs (Figure 1d), suggesting avulsions that do occur are smaller in scale than those on deltas with thin ice (e.g., between branches of a bifurcation or relocating part of a channel rather than the entire channel). These smaller scale avulsions do not result in complete abandonment of existing entrenched channels, resulting in more channels active at one time than on a delta with no ice.

4. Delta Growth and Structure

Increased channel persistence affects large-scale delta growth patterns, limiting deposition to particular areas of the shoreline and increasing rugosity. The presence of permafrost significantly increases shoreline rugosity (Figure 3a) by limiting lateral channel mobility, thus focusing deposition at fewer, more stable channel mouths. However, shoreline roughness does not depend on permafrost erodibility. For ice-covered deltas, shoreline roughness increases significantly with ice thickness and ice extent (Figures 3b, 3c, 3e, and 3f). Reductions in channel bed aggradation and channel mobility create elongate channels and discrete, isolated areas of deposition at the shoreline. These effects of fast ice and permafrost are like those of cohesive sediment, which tends to create discrete delta lobes and rougher shorelines (Hoyal & Sheets, 2009; Liang, Voller, & Paola, 2015), though the mechanisms for enhancing channel stability differ.

More persistent channels also influence deposition offshore. The presence of slightly resistant permafrost results in more offshore deposition, but as permafrost erodibility decreases, less sediment is available for

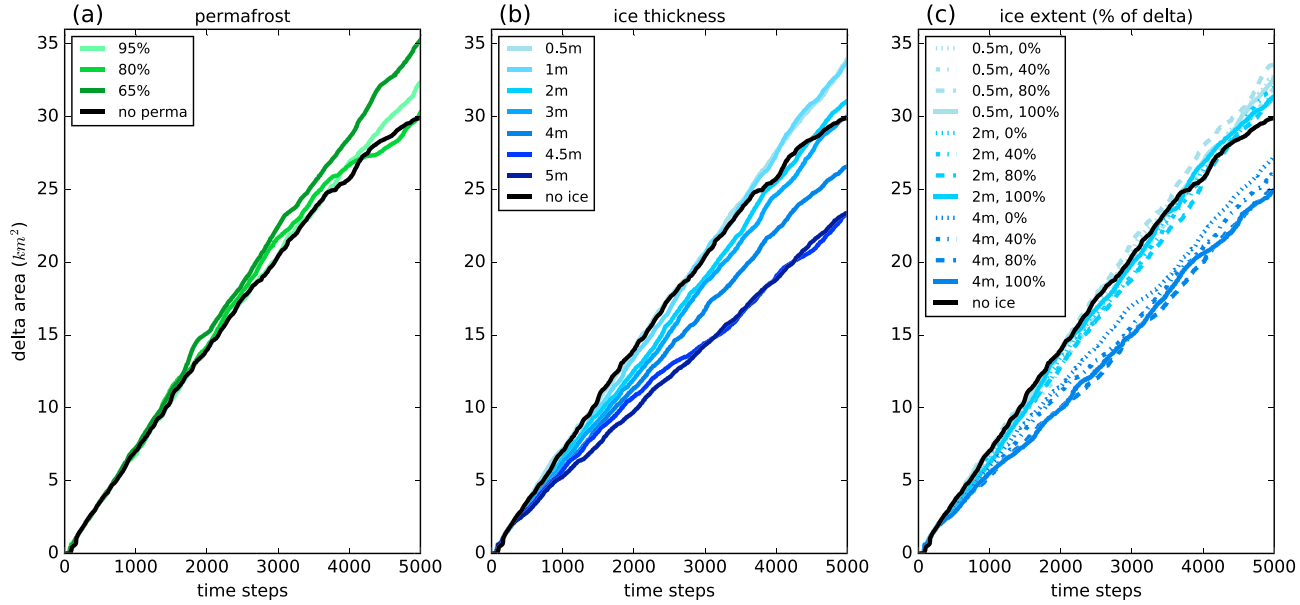

Figure 4. Time series of delta area for (a) permafrost erodibility, (b) maximum ice thickness, and (c) maximum ice extent.

transport to the coastal ocean (Figure 5d). With very low erodibilities (Figures S3 and S4), erosion can become so difficult that less sediment is delivered offshore than with no permafrost. Deltas with ice cover route more sediment offshore as increased channel velocities limit in-channel deposition and channels extend beyond the delta, incising into the basin (Figures 3e and 5i). This behavior is consistent with observations of sub–ice channel extension, incision, and sediment transport on the Mackenzie (Hill et al., 2001) and Yukon (Dupre, 1979) deltas and results in decreasing progradation rates with increasing ice thickness as more sediment is lost to the ocean. Deltas covered with thick ice have smaller final subaerial extents for the same volume of sediment input (Figures 4b, 3e, and 5i). There is no clear relationship between delta growth rate and permafrost erodibility (Figure 4a) or ice extent (Figure 4c).

An increase in offshore deposition on ice-covered deltas creates a feature resembling the 2-m-deep ramp observed off the coast of many Arctic deltas (Macdonald & Yu, 2006; Reimnitz, 2002), consistent with the hypothesis that these ramps form as flow constriction leads to offshore deposition until the bed reaches the base of the ice (Reimnitz, 2002). In our experiments, the largest “shelves” occur with intermediate ice thicknesses (i.e., 2–3 m; Figures 3f and 5h). Thin ice does not constrict flow enough to promote offshore deposition, and thick ice limits the space available for offshore transport between the bed and the ice. Sediment transport to the shoreline is maximized for intermediate ice thicknesses (Figure S2). Ice extent does not influence offshore deposition (Figure 5f). Onshore, thick ice increases median subaerial delta elevations (Table S2; Figures 5b and 5c), as water level backup results in increased flooding and overbank deposition (Figure S2). Subaerial elevation distributions are significantly different with thicker ice cover (1, 4, 4.5, and 5 m [Figure 5b] and 4 m, 40% and 80% [Figure 5c]) relative to ice-free deltas. Subaerial elevation distributions do not change significantly with permafrost erodibility (Figure 5a).

5. Implications for Future Coastal Change

Our results suggest that ice and permafrost affect channel mobility, influence the number of distributary channels, increase shoreline roughness, and enhance offshore deposition. Thick ice cover also decreases delta progradation and increases overbank deposition rates. Ice cover appears to have a stronger influence on modeled delta dynamics and morphology than permafrost, and ice thickness to be a more important driver than ice extent. This suggests that ice thickness may be a more important factor in understanding the response of natural Artic river deltas to climate change compared to the extent of ice cover during spring floods.

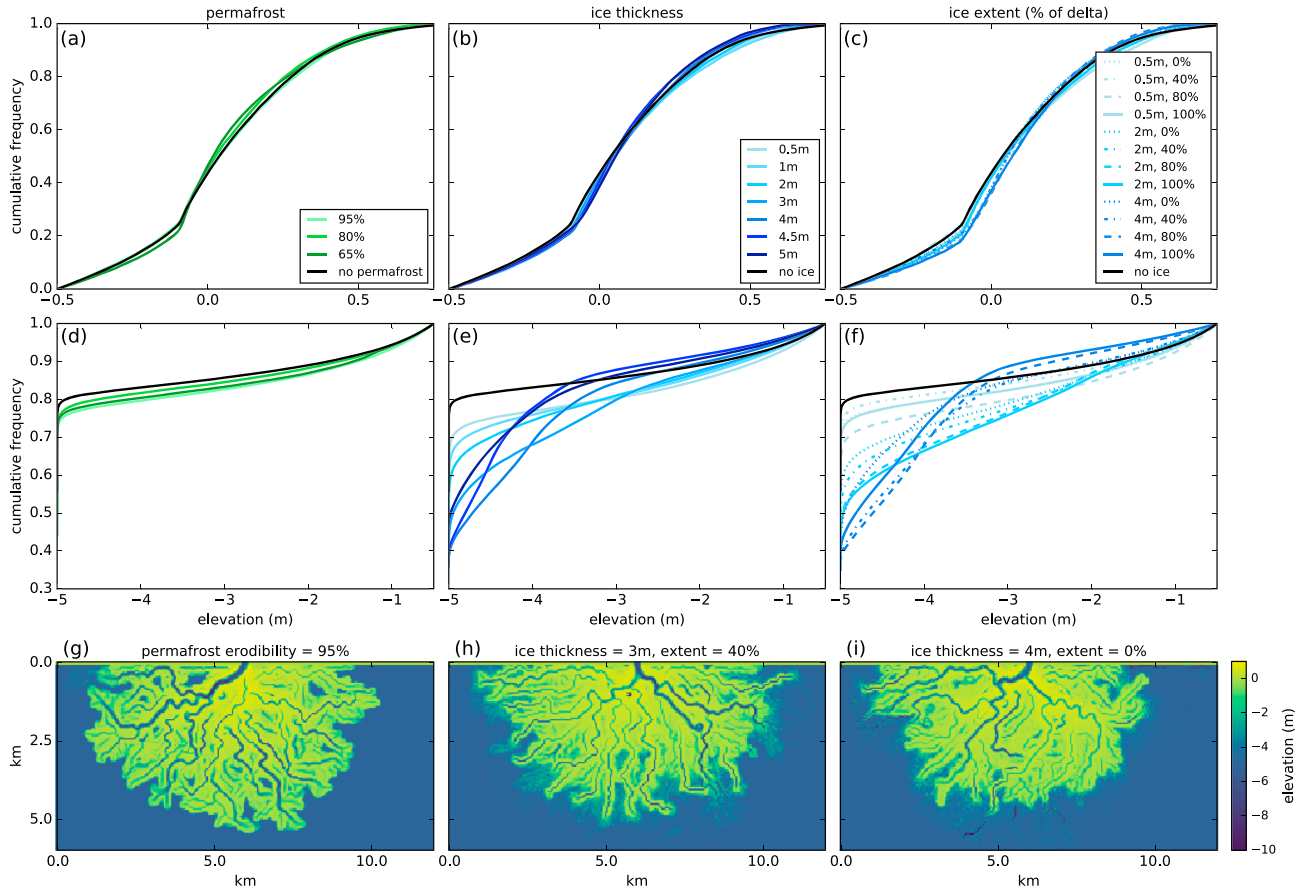

Figure 5. Empirical cumulative distribution functions of final delta elevations. (a)–(c) include subaerial elevations (>−0.5 m) and (d)–(f) include subaqueous elevations (<−0.5 m). Elevation maps for example runs with (g) permafrost erodibility of 95%, (h) maximum ice thickness of 3 m and extent of 40% (arrow highlights offshore deposition), and (i) maximum ice thickness of 4 m and extent of 0% (arrow highlights a preserved abandoned channel).

As sea ice retreats or permafrost thaws, the stabilizing effects of ice and permafrost will decrease and channel networks may become more dynamic. Our results suggest that a decrease in ice present at the time of the spring flood may result in channel networks that are more widely distributed across the delta, with increased channel mobility and more large-scale (e.g., whole channel and/or across-delta) avulsions. Recent studies have also suggested that an earlier retreat of sea ice relative to the timing of the spring snowmelt flood would reduce the amount of overbank flooding on the Mackenzie delta (Emmerton et al., 2007), thus limiting the storage of water, sediment, and nutrients in the delta plain and instead routing riverine fluxes directly to the coast. This reduction in storage, combined with increased reworking of the delta surface as suggested by our study, may alter the magnitude and timing of the delivery of materials such as carbon (Gustafsson et al., 2011; Rowland et al., 2010) or mercury (Schuster et al., 2018) to the coastal ocean. Further, a reduction in overbank flooding with a decrease in ice cover, supported by our study, would likely reduce the rate of vertical aggradation, limiting delta ability to keep up with sea level rise.

This study represents a first attempt to characterize the dynamics of Arctic river deltas over larger space and time scales than are possible from remote sensing and field observations. While our results complement existing observations (Dupre, 1979; Emmerton et al., 2007; Hill et al., 2001; Macdonald & Yu, 2006; Reimnitz, 2002), they also identify questions for future research. Interactions between ice cover, permafrost, and additional variables including temporal changes in ice extent at the start of floods, sea level, and flood discharge should be investigated. By generating basic understanding of the influence of ice cover and permafrost on delta dynamics, our study provides a valuable foundation for this future work and emphasizes the need for collection of additional observational data on channel mobility rates, water and sediment fluxes, and depositional patterns on Arctic river deltas under various changing ice and permafrost conditions.

Acknowledgments

This work was funded by the HiLAT project through DOE's Regional and Global Climate Modeling program. The data can be found in Table S4. This study benefitted from discussions with Man Liang, Brad Murray, Irina Overeem, and Todd Ringler.

References

ACIA (2004). *Impacts of a warming Arctic: Arctic Climate Impact Assessment* (139 pp.). Cambridge: Cambridge University Press.

Attar, S., & Li, S. S. (2012). Data-fitted velocity profiles for ice-covered rivers. *Canadian Journal of Civil Engineering*, *39*(3), 334–338. https://doi.org/10.1139/l2012-001

Barnhart, K. R., Miller, C. R., Overeem, I., & Kay, J. E. (2016). Mapping the future expansion of Arctic open water. *Nature Climate Change*, *6*(3), 280–285. https://doi.org/10.1038/nclimate2848

Dupeyrat, L., Costard, F., Randriamazaoro, R., Gailhardis, E., Gautier, E., & Fedorov, A. (2011). Effects of ice content on the thermal erosion of permafrost: Implications for coastal and fluvial erosion. *permafrost and periglacial processes*, *22*(2), 179–187. https://doi.org/10.1002/ppp.722

Dupre, W. R. (1979). *Yukon Delta coastal processes study Rep*. Boulder, CO: National Oceanic and Atmospheric Administration.

Emmerton, C. A., Lesack, L. F. W., & Marsh, P. (2007). Lake abundance, potential water storage, and habitat distribution in the Mackenzie River Delta, western Canadian Arctic. *Water Resources Research*, *43*, W05419. https://doi.org/10.1029/2006WR005139

Gustafsson, O., van Dongen, B. E., Vonk, J. E., Dudarev, O. V., & Semiletov, I. P. (2011). Widespread release of old carbon across the Siberian Arctic echoed by its large rivers. *Biogeosciences*, *8*(6), 1737–1743. https://doi.org/10.5194/bg-8-1737-2011

Hill, P. R., Lewis, C. P., Desmarais, S., Kauppaymuthoo, V., & Rais, H. (2001). The Mackenzie Delta: sedimentary processes and facies of a high-latitude, fine-grained delta. *Sedimentology*, *48*(5), 1047–1078. https://doi.org/10.1046/j.1365-3091.2001.00408.x

Hoyal, D., & Sheets, B. A. (2009). Morphodynamic evolution of experimental cohesive deltas. *Journal of Geophysical Research*, *114*, F02009. https://doi.org/10.1029/2007JF000882

Intergovernmental Panel on Climate Change (2013). *Climate Change 2013: The physical science Basis Rep* (1535 pp.). Cambridge, UK and New York: Cambridge University Press.

Jorgenson, M. T., Shur, Y. L., & Pullman, E. R. (2006). Abrupt increase in permafrost degradation in Arctic Alaska. *Geophysical Research Letters*, *33*, L02503. https://doi.org/10.1029/2005GL024960

Lachenbruch, A. H., & Marshall, B. V. (1986). Changing climate—Geothermal evidence from permafrost in the Alaskan Arctic. *Science*, *234*(4777), 689–696. https://doi.org/10.1126/science.234.4777.689

Lau, Y. L., & Krishnappan, B. G. (1985). Sediment transport under ice cover. *Journal of Hydraulic Engineering-Asce*, *111*(6), 934–950. https://doi.org/10.1061/(ASCE)0733-9429(1985)111:6(934)

Liang, M., Geleynse, N., Edmonds, D. A., & Passalacqua, P. (2015). A reduced-complexity model for river delta formation - Part 2: Assessment of the flow routing scheme. *Earth Surface Dynamics*, *3*(1), 87–104. https://doi.org/10.5194/esurf-3-87-2015

Liang, M., Kim, W., & Passalacqua, P. (2016). How much subsidence is enough to change the morphology of river deltas? *Geophysical Research Letters*, *43*, 10,266–10,276. https://doi.org/10.1002/2016GL070519

Liang, M., Van Dyk, C., & Passalacqua, P. (2016). Quantifying the patterns and dynamics of river deltas under conditions of steady forcing and relative sea level rise. *Journal of Geophysical Research: Earth Surface*, *121*, 465–496. https://doi.org/10.1002/2015JF003653

Liang, M., Voller, V. R., & Paola, C. (2015). A reduced-complexity model for river delta formation—Part 1: Modeling deltas with channel dynamics. *Earth Surface Dynamics*, *3*(1), 67–86. https://doi.org/10.5194/esurf-3-67-2015

Lotsari, E., Kasvi, E., Kamari, M., & Alho, P. (2017). The effects of ice cover on flow characteristics in a subarctic meandering river. *Earth Surface Processes and Landforms*, *42*(8), 1195–1212. https://doi.org/10.1002/esp.4089

Macdonald, R. W., & Yu, Y. (2006). The Mackenzie Estuary of the Arctic Ocean. In P. J. Wangersky (Ed.), *Estuaries* (Vol. 5, pp. 91–120). Berlin, Heidelberg: Springer. https://doi.org/10.1007/698_5_027

Murray, A. B. (2003). Contrasting the goals, strategies, and predictions associated with simplified numerical models and detailed simulations. *Prediction in Geomorphology*, *135*, 151–168. https://doi.org/10.1029/135GM11

Overeem, I., Anderson, R. S., Wobus, C. W., Clow, G. D., Urban, F. E., & Matell, N. (2011). Sea ice loss enhances wave action at the Arctic coast. *Geophysical Research Letters*, *38*, L17503. https://doi.org/10.1029/2011GL048681

Proshutinsky, A., Pavlov, V., & Bourke, R. H. (2001). Sea level rise in the Arctic Ocean. *Geophysical Research Letters*, *28*(11), 2237–2240. https://doi.org/10.1029/2000GL012760

Randriamazaoro, R., Dupeyrat, L., Costard, F., & Gailhardis, E. C. (2007). Fluvial thermal erosion: Heat balance integral method. *Earth Surface Processes and Landforms*, *32*(12), 1828–1840. https://doi.org/10.1002/esp.1489

Reimnitz, E. (2002). Interactions of river discharge with sea ice in proximity of Arctic deltas: A review. *Polarforschung*, *70*, 123–134.

Robert, A., & Tran, T. (2012). Mean and turbulent flow fields in a simulated ice-covered channel with a gravel bed: some laboratory observations. *Earth Surface Processes and Landforms*, *37*(9), 951–956. https://doi.org/10.1002/esp.3211

Rowland, J. C., Jones, C. E., Altmann, G., Bryan, R., Crosby, B. T., Hinzman, L. D., et al. (2010). Arctic landscapes in transition: Responses to thawing permafrost. *Eos, Transactions American Geophysical Union*, *91*(26), 229–230. https://doi.org/10.1029/2010EO260001

Schuster, P. F., Schaefer, K. M., Aiken, G. R., Antweiler, R. C., Dewild, J. F., Gryziec, J. D., et al. (2018). Permafrost stores a globally significant amount of mercury. *Geophysical Research Letters*, *45*, 1463–1471. https://doi.org/10.1002/2017GL075571

Searcy, C., Dean, K., & Stringer, W. (1996). A river-coastal sea ice interaction model: Mackenzie River Delta. *Journal of Geophysical Research*, *101*(C4), 8885–8894. https://doi.org/10.1029/96JC00120

Simmonds, I. (2015). Comparing and contrasting the behaviour of Arctic and Antarctic sea ice over the 35 year period 1979-2013. *Annals of Glaciology*, *56*(69), 18–28. https://doi.org/10.3189/2015AoG69A909

Slater, A. G., & Lawrence, D. M. (2013). Diagnosing present and future permafrost from climate models. *Journal of Climate*, *26*(15), 5608–5623. https://doi.org/10.1175/JCLI-D-12-00341.1

Smith, B. T., & Ettema, R. (1997). Flow resistance in ice-covered alluvial channels. *Journal of Hydraulic Engineering-Asce*, *123*(7), 592–599. https://doi.org/10.1061/(ASCE)0733-9429(1997)123:7(592)

Sui, J. Y., Wang, J., He, Y., & Krol, F. (2010). Velocity profiles and incipient motion of frazil particles under ice cover. *International Journal of Sediment Research*, *25*(1), 39–51. https://doi.org/10.1016/S1001-6279(10)60026-1

Toniolo, H., Vas, D., Prokein, P., Kenmitz, R., Lamb, E., & Brailey, D. (2013). Hydraulic characteristics and suspended sediment loads during spring breakup in several streams located on the National Petroleum Reserve in Alaska, USA %. *Natural Resources*, *04*(02), 220–228. https://doi.org/10.4236/nr.2013.42028

Tsytovich, N. A. (1975). *The mechanics of frozen ground*. New York: McGraw-Hill.

Walker, H. J. (1998). Arctic deltas. *Journal of Coastal Research*, *14*(3), 718–738.

Walker, H. J., & Hudson, P. F. (2003). Hydrologic and geomorphic processes in the Colville River delta, Alaska. *Geomorphology*, *56*(3-4), 291–303. https://doi.org/10.1016/S0169-555X(03)00157-0

Wang, J., Sui, J. Y., & Karney, W. K. (2008). Incipient motion of non-cohesive sediment under ice cover—An experimental study. *Journal of Hydrodynamics*, *20*(1), 117–124. https://doi.org/10.1016/S1001-6058(08)60036-0

Williams, P. J., & Smith, M. W. (1991). *The Frozen Earth*. New York: Cambridge University Press.

References From the Supporting Information

Shaw, J. B., Wolinsky, M. A., Paola, C., & Voller, V. R. (2008). An image-based method for shoreline mapping on complex coasts. *Geophysical Research Letters*, *35*, L12405. https://doi.org/10.1029/2008GL033963

Wickert, A. D., Martin, J. M., Tal, M., Kim, W., Sheets, B., & Paola, C. (2013). River channel lateral mobility: metrics, time scales, and controls. *Journal of Geophysical Research: Earth Surface*, *118*, 396–412. https://doi.org/10.1029/2012JF002386

Wolinsky, M. A., Edmonds, D. A., Martin, J., & Paola, C. (2010). Delta allometry: Growth laws for river deltas. *Geophysical Research Letters*, *37*, L21430. https://doi.org/10.1029/2010GL044592